J Comput Aided Mol Des (2016) 30:569–581
DOI 10.1007/s10822-016-9934-z

A computational docking study on the pH dependence of peptide binding to HLA-B27 sub-types differentially associated with ankylosing spondylitis

Onur Serçinoğlu[1] · Gülin Özcan[1] · Zeynep Kutlu Kabaş[1] · Pemra Ozbek[1]

Received: 26 March 2016 / Accepted: 4 August 2016 / Published online: 9 August 2016

Abstract A single amino acid difference (Asp116His), having a key role in a pathogenesis pathway, distinguishes HLA-B*27:05 and HLA-B*27:09 sub-types as associated and non-associated with ankylosing spondylitis, respectively. In this study, molecular docking simulations were carried out with the aim of comprehending the differences in the binding behavior of both alleles at varying pH conditions. A library of modeled peptides was formed upon single point mutations aiming to address the effect of 20 naturally occurring amino acids at the binding core peptide positions. For both alleles, computational docking was applied using Autodock 4.2. Obtained free energies of binding (FEB) were compared within the peptide library and between the alleles at varying pH conditions. The amino acid preferences of each position were studied enlightening the role of each on binding. The preferred amino acids for each position of pVIPR were found to be harmonious with experimental studies. Our results indicate that, as the pH is lowered, the capacity of HLA-B*27:05 to bind peptides in the library is largely lost. Hydrogen bonding analysis suggests that the interaction between the main anchor positions of pVIPR and their respective binding pocket residues are affected from the pH the most, causing an overall shift in the FEB profiles.

Keywords Computational molecular docking · Autodock 4.2 · HLA docking · Peptide docking · HLA-B27 · pH change · Cross-presentation

Introduction

T lymphocytes recognize antigen fragments presented by Major Histocompatibility Complex (MHC) proteins on the surface of professional antigen presenting cells (APCs). These fragments are short peptides derived from proteins in the cytosol (endogenous proteins) or internalized from the extracellular environment (exogenous proteins). Endogenous and exogenous proteins are processed in two different pathways to yield peptides that bind to either MHC Class I or Class II proteins. Different classes of peptide-loaded MHC molecules (pMHC proteins) are recognized by different T cell subsets: MHC I molecules are recognized by CD8+ cytotoxic T-cells whereas MHC II molecules are recognized by CD4+ T cells [1].

In the MHC I pathway, the proteasome complex in the cytosol degrades the antigen into short peptides which are taken into the Endoplasmic Reticulum (ER) with the help of a dimeric protein, which is known as Transported Associated with Antigen Processing (TAP). The peptides are then bound by MHC Class I proteins with the help of the peptide-loading complex in the ER and later transported to the cell surface [2]. On the other hand, in the MHC II pathway, extracellular protein is taken up via

Electronic supplementary material The online version of this article (doi:10.1007/s10822-016-9934-z) contains supplementary material, which is available to authorized users.

✉ Pemra Ozbek
pemra.ozbek@marmara.edu.tr

Onur Serçinoğlu
onur.sercinoglu@marmara.edu.tr

Gülin Özcan
glnozcan@gmail.com

Zeynep Kutlu Kabaş
kutluzeynep@gmail.com

[1] Faculty of Engineering, Department of Bioengineering, Goztepe Campus, MC-373, Marmara University, 34722 Goztepe, Istanbul, Turkey

endocytosis, proteolytically degraded into peptides and bound by MHC II proteins in a specialized endosome (MIIC, MHC class II containing compartment).

The molecular players taking roles in both pathways are distinct, however this segregation of pathways is not absolute: loading of MHC I proteins with exogenous antigens is also possible [3–5]. This phenomenon is called *cross-presentation* or *cross-priming* and was shown to be necessary in inducing Class I restricted CD8+ cytotoxic T-cell responses against viruses or tumors where dendritic cells are not directly infected [6].

Two major pathways have been proposed to explain the molecular mechanisms responsible for cross-presentation: cytosolic and vacuolar pathways. The difference between these two pathways is the subcellular location where antigen processing and peptide loading takes place. In the cytosolic (or proteasome-dependent) pathway, internalized antigens are transferred to the cytosol from endosomes and peptide processing is achieved by the proteasome machinery. Resulting peptides are then loaded onto MHC I molecules in the ER. In the vacuolar (or proteasome-independent) pathway, the antigen is cleaved into peptides by proteases and bound by MHC I molecules in the endosome [7]. Dendritic cells have been identified as the most effective cross-presenting cell type as there is proof for their ability of transporting external antigens into the cytosol as well as performing peptide loading onto MHC I molecules in the endosomes [8].

For successful peptide-loading onto MHC I in the endosomes, peptide MHC I molecules should be available in a peptide-loadable state at the location of peptide loading. In the endosomes, the pH is acidic (at around 5) [9] and the proteolytic degradation is achieved by proteases that have acidic pH optima. Acidic pH also helps in the dissociation of the MHC II protein from the invariant chain (Ii or CD74), which occupies the binding groove of MHC II proteins and prevents peptide binding in the ER [10]. In contrast, the pH in the cytosol is neutral [11], meaning that MHC Class I and Class II proteins normally bind peptides under different pH conditions. This pH dependence is supported by studies that show MHC II molecules are significantly more stable under low pH conditions than MHC I molecules [12]. Moreover, low pH may also degrade the antigen and possible MHC I epitopes by activating endosomal proteases [13]. Further support for high pH requirement came from studies that demonstrate lower levels of lysosomal proteases [14] and less acidic pH due to the action of NOX2 enzyme [15, 16] in dendritic cell endosomes. On the other hand, acidic pH was also proposed to facilitate peptide detachment from MHC I molecules that are recycled back from the cell surface [17]. Empty MHC I molecules would then be loaded with new peptides in the endosomes. Acidic pH conditions were also shown to enhance binding of some peptides to MHC I molecules [18]. Furthermore, evidence is increasing for the involvement of Class II peptide-loading machinery (invariant chain assisted loading) in MHC I peptide loading in endosomes [19–21].

Acidic pH conditions may also be relevant for peptide-loading/exchange following exit from the ER. Peptide-loading in the post-ER compartments such as the slightly acidic Trans Golgi Network (TGN) was proposed as a possible "rescue" mechanism for unfolded or incorrectly folded MHC I molecules [22, 23]. This mechanism of peptide-loading may also be allele-dependent since it was demonstrated for HLA-B27 (HLA: Human Leukocyte Antigen) and HLA-B51 alleles of human MHC I molecules but not for the HLA-A2 allele [24, 25]. Given the associations of the HLA-B27 and HLA-B51 alleles with ankylosing spondylitis (AS) and Behçet's Disease, respectively [26–30] investigating the structural peptide-binding behavior of HLA proteins under acidic conditions may help explain possible underlying molecular mechanisms involved in the development of these autoimmune diseases.

Obtaining a structural overview of peptide binding to HLA proteins, and possibly also its pH dependence, experimentally would require the structural determination of an enormous number of peptide-MHC complex possibilities. This is a time consuming and an expensive process, hence computational methods are preferred in the study of peptide binding to MHC molecules. Mostly focusing on the identification of the candidate peptides, various techniques have been used and details can be found in several reviews [31–33]. Comparisons of available data and servers are also available [34, 35]. Computational molecular docking methods are widely used and constantly being developed to predict the actual binding behavior while exploring the possibility of interaction sites on protein structures. Based on X-ray structure data retrieved from the Protein Data Bank (PDB) [36], peptides are computationally placed in the binding grooves of HLA molecules using various docking techniques. The accuracy of the docking performance is measured in terms of Root Mean Square Distance (RMSD) obtained by comparing the docked conformations of the peptides to their original bound conformations, where a correct docking result is defined as a complex having an RMSD of less than 2.0 Å based on the known experimental structure.

Previously, Patronov et al. [37] studied the binding behavior of four HLA-DP protein structures (class II MHC proteins) at different pH using molecular docking with a virtual combinatorial peptide library approach. In this work, we used the same approach to study the pH dependence of peptide binding behaviors of HLA-B*27:05 and HLA-B*27:09 alleles at pH 5, 6 and 7 in a comparative manner. These two alleles differ at amino acid position 116

which is located at the peptide binding groove [38]. HLA-B*27:05 has an aspartic acid (Asp), while B*27:09 has a histidine (His) at this position. The two alleles are also differentially associated with the ankylosing spondylitis disease. While HLA-B*27:05 is associated with AS, HLA-B*27:09 is not [39].

The peptide binding groove of HLA class 1 is a well-defined cavity formed between two α-helices (α1 and α2) where the floor of the groove is formed by a β-sheet structure. The binding site of HLA-B*27 comprises 6 pockets (A–F) [40] and the peptide primary anchor residues are located at positions P2 and the C-terminal, P9. Details of the pockets and the interacting peptide residues are given in Fig. 1. Both alleles interact with T cells differently although they share the same peptide repertoire. It is shown that the dynamic properties of the two complexes differ drastically [41].

To start with, we generated a library of nonameric peptide structures corresponding to 172 different peptide sequences for each allele at pH 5, 6 and 7 by taking template peptide structures from the PDB (PDB IDs of 1OF2 and 1OGT (A&B forms refer to canonical and non-canonical forms respectively) and modifying the protonation states of amino acids according to pH. Protonation states of amino acid residues of the HLA molecules were also modified according to the respective pH. Then, we generated peptide-MHC complexes for each peptide using Autodock 4.2 docking software [42] and obtained free

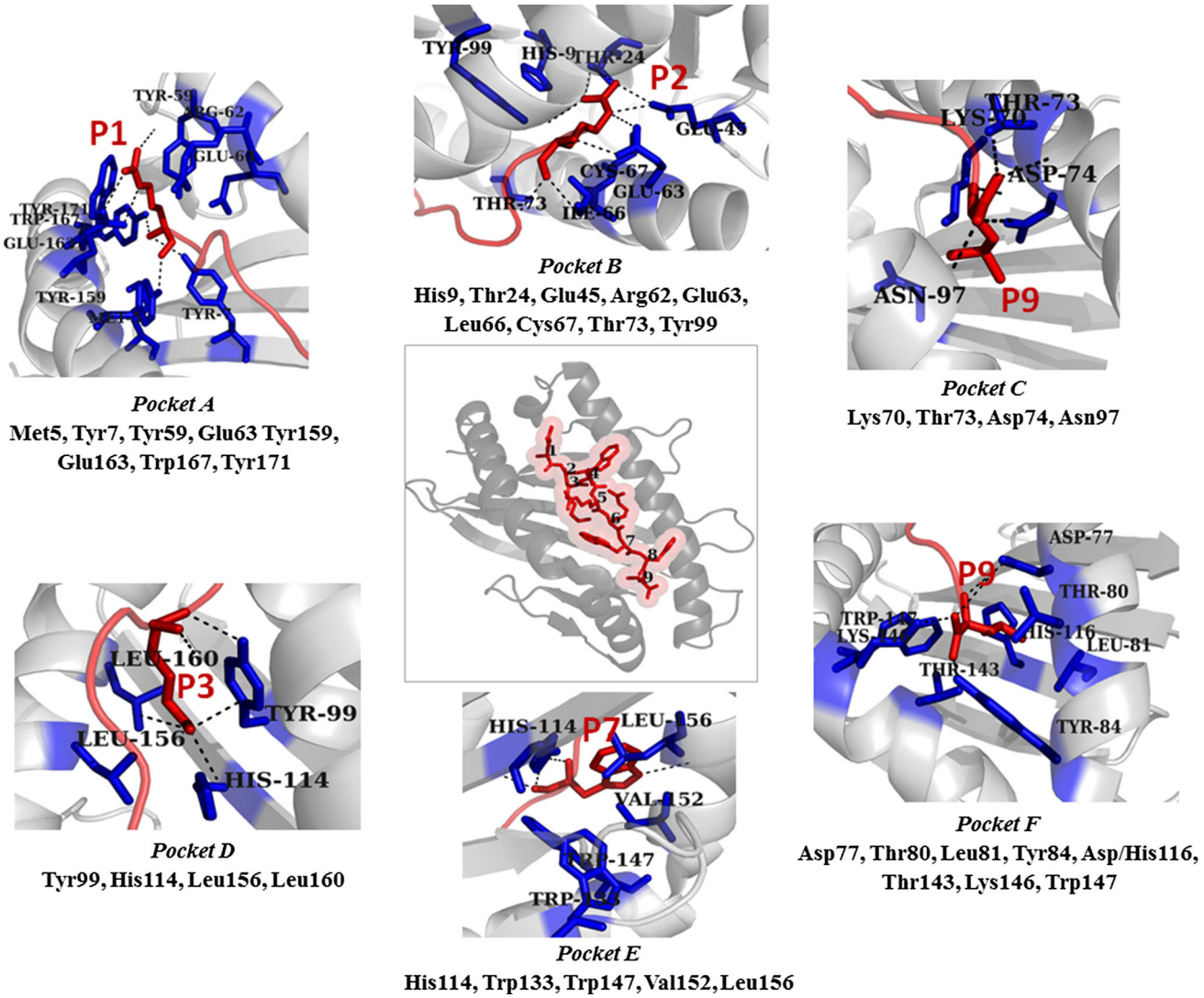

Fig. 1 Binding groove pockets and the interacting peptide residues are shown individually on the structure of HLA-B*27:09 (1OF2) [43]. The *middle panel* shows the binding groove in *gray* and the peptide in *red*. The peptide residues are labeled (*1–9*). The *side panels* display binding pockets and the peptide residues that they are interacting with. Peptide is shown in *red*, *blue lines* indicate the pocket residues and the peptide residues that they are interacting with are shown as *red sticks*. Hydrogen bonds are shown in *black dashed lines*. The images were prepared using Pymol [44]

energies of binding FEB values estimated by Autodock 4.2. In addition, an analysis of hydrogen bonds and pair-wise interaction energies between peptide and HLA binding groove amino acids was performed in order to identify the residues that are affected by the change in pH the most.

Materials and methods

Input data

The initial dataset used in the study is composed of pairs of HLA-B*27:05 and HLA-B*27:09 sub-types retrieved from the PDB [36]. Table 1 details the structures used in this study.

The peptides bound to structures of HLA-B*27 sub-types in this study (Table 1) are all nonapeptides derived from various sources: vasoactive intestinal peptide type 1 receptor (pVIPR, residues 400–408); totally artificial m9; a member of epidermal growth factor early response gene (self-peptide, TIS); latent membrane protein 2 of Epstein-Barr virus (pLMP2, residues 236–244); a peptide from cathepsin A (pCatA, residues 2–10). pVIPR is known to be accommodated in two different conformations when bound to B*27:05 [canonical (A) and non-canonical (B)] intrinsically [43]. This dual conformation is reflected on the backbone torsion angles of the peptide (see Supplementary Figure 1).

Peptide library formation

Further detailed analysis on varying pH conditions using a combinatorial library was advanced on structures 1OF2 and 1OGT [43] bound to the same peptide, pVIPR (RRKWRRWHL/Arg–Arg–Lys–Trp–Arg–Arg–Trp–His–Leu). This peptide was used to create a virtual combinatorial peptide library. For 1OGT, both canonical (pVIPR_A) and non-canonical (pVIPR_B) conformations were taken into account. Each amino acid position of the peptide was mutated systematically into 20 naturally occurring amino acids while the rest of the positions were kept using the Mutagenesis tool of PyMol [44]. This leads to a total of 172 unique peptide structures for each conformation (19 amino acids $\times$ 9 positions + 1 original ligand). Following the formation of the library, peptides were energy-minimized while keeping the HLA macromolecule rigid.

Adjustment of pH conditions

Aiming to investigate the effect of pH on the docking results, the conformations of the structures at varying pH (5.0, 6.0 and 7.0) were adjusted using the CHARMM force field setting of ProPka [45], which takes the local environment of the residues into account. The protonation states of the residues affected (His, Asp, Glu) at these pH are given in Fig. 2 and Supplementary Table 1 for both alleles. For simplicity, only the residues that display varying protonation states are shown.

Molecular docking protocol

Autodock 4.2 [42] was used to model the peptide binding in structures of HLA-B*27:05 and HLA-B*27:09 sub-types. Lamarckian genetic algorithm was employed, while the scoring function takes van der Waals, dispersion/repulsion, hydrogen bonding, electrostatics, desolvation interactions and the change in torsional free energy into account. In order to limit the computational time, all coordinates were kept fixed except the peptide residues. Since we were interested in the effect of pH only, the conformation search space in Autodock 4.2 was set according to the already known HLA binding groove. The docking grid size was defined as a cuboid with dimensions of 72 Å $\times$ 40 Å $\times$ 52 Å. The number of GA runs and maximum number of evaluation parameters were varied in order to find the best conformation based on the lowest RMSD and FEB values. Various combinations were employed on the structures bound to pVIPR and the results are shown in Supplementary Tables 2–4. Accordingly, the combination of parameters giving the best docking results in terms of both FEB and RMSD values were chosen that is valid for both alleles (HLA-B*27:05 and HLA-B*27:09) in order to be consistent for the rest of the study. As long as the RMSD values were below 2.0 Å, assuring the correctness of docking, the rest of the choice was mainly driven by the FEB value. As a result, all the settings were kept to their default values while taking the number of Genetic algorithm (GA) runs as 50, the number of torsions

Table 1 PDB accession codes for crystal structures of the proteins HLA-B*27:05 and HLA-B*27:09 with different bound peptides selected for the study

HLA-B*27:09	HLA-B*27:05	Peptide	Origin	Resolution (Å)
1OF2	1OGT (A&B)	pVIPR (RRKWRRWHL)	Self	2.20/1.47
1K5N	1JGE	m9 (GRFAAAIAK)	Model	1.09/2.10
1W0W	1W0V	TIS (RRLPIFSRL)	Self	2.10/2.27
1UXW	1UXS	pLMP2 (RRRWRRLTV)	Viral	1.71/1.55
3BP7	3BP4	pCatA (IRAAPPPLF)	Self	1.80/1.85

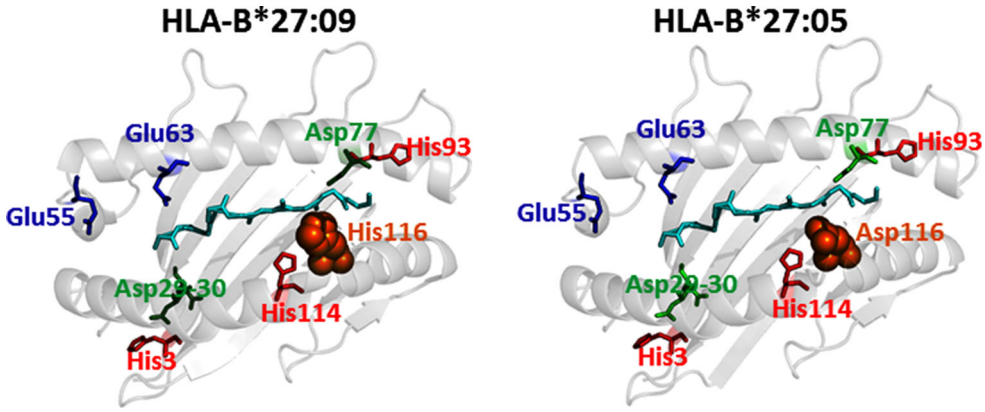

Fig. 2 Binding groove residues with varied protonation states according to the pH studied (pH5, pH6, pH7) are shown on structures of both HLA-B*27:05 (1OGT_A) and HLA-B*27:09 (1OF2) [43]. Protein structures are shown in *gray cartoon* representation, peptide as *cyan sticks*, His as *red sticks*, Asp as *green sticks*, Glu as *dark blue sticks* and the polymorphic residue (His/Asp116) as *orange spheres*. The images were prepared using Pymol [44]

as 16 and the maximum number of evaluations as 25,000,000. The affinity between the receptor and the ligand was calculated in terms of Gibbs FEB and the pose with the lowest FEB was taken into account out of 50 independent GA runs for each peptide. In the rest of the study, dockings were performed using these parameters.

Normalized free energy of binding calculations for peptide library docking

The FEB obtained from the outputs were normalized based on the average calculated on a position dependent basis within each allele [46]. Since the positive FEBs correspond to non-binding peptides, they were given a penalty score of −10,000. The formula used to calculate normalized FEB is given as,

$$\mathrm{FEB_{i,norm}} = \frac{\mathrm{FEB_i} - \mathrm{FEB_{avg}}}{\mathrm{FEB_{max}} - \mathrm{FEB_{min}}} \quad (1)$$

where FEB_i is the binding energy of the i-th peptide, FEB_{avg} is the average for a given position, FEB_{max} and FEB_{min} the maximum and minimum FEBs, respectively. The obtained values were multiplied by (−1) for ease of presentation. Hence, the positive normalized FEBs correspond to preferred amino acids and negative normalized FEBs correspond to non-preferred residues in the tables given in the "Results and discussion" section.

Experimental peptide binding data

Peptide binders to both HLA-B*27:05 and HLA-B*27:09 subtypes were collected from the Immune Epitope Database (IEDB) [47] and data from Schittenhelm et al. [48]. Only nonamers were taken into account. The list of binders was used to construct an amino acid preference matrix which includes the number of occurrences of each amino acid at each peptide position. This matrix was then normalized to enable an easier qualitative comparison between the amino acid preferences obtained using normalized FEB values from Autodock 4.2.

Hydrogen bond analysis on docking results

Hydrogen bonds between the peptide and the binding groove residues in each docked peptide-HLA complex were computed using HBonanza [49]. A bond angle of 30° and a distance cut-off of 3.0 Å were used [50]. The resulting output files were then parsed and analyzed using custom python scripts in order to identify the binding groove/peptide residues which are affected the most from the pH change for each B27 sub-type.

Results and discussion

Molecular redocking of peptides at varying pH conditions

Initially, we applied our protocol to the rebuilding of the already existing HLA*B-27:05/HLA*B-27:09—(non-americ) peptide complexes from the Protein Data Bank (see Table 1 in "Materials and methods" section) by docking peptides extracted from HLA-B*27 complexes back into their respective binding grooves. Each redocking was performed four times at each pH condition (details of the results are given in Table 2; Fig. 3). The RMSD values between the native peptide conformation and the peptide conformation suggested by the lowest energy solution of Autodock 4.2 were calculated where the maximum RMSD observed is 0.93 ± 0.02 Å (Supplementary Table 5). Since

Table 2 Autodock 4.2 FEB scores (kcal/mol) obtained at the end of redocking of HLA-B*27:05 and HLA-B*27:09 alleles along with the allele-wise differences in the free energies of binding at each pH condition

	Peptide	$\Delta G_{B*27:09}$ (kcal/mol)		$\Delta G_{B*27:05}$ (kcal/mol)		$\Delta\Delta G_{B*27:09-B*27:05}$ (kcal/mol)	
						This work	Experimental data from [51][a]
pH5	pVIPR (RRKWRRWHL)	1OF2	−17.26 ± 0.33	1OGT_A	−17.32 ± 0.23	−0.05 ± 0.56	
				1OGT_B	−18.00 ± 0.28		
	m9 (GRFAAAIAK)	1K5N	−13.14 ± 0.73	1JGE	−14.16 ± 0.40	−1.02 ± 1.13	
	TIS (RRLPIFSRL)	1W0W	−15.95 ± 0.04	1W0V	−13.97 ± 0.12	1.99 ± 0.16	
	pLMP2(RRRWRRLTV)	1UXW	−15.13 ± 0.02	1UXS	−17.51 ± 0.11	−2.39 ± 0.13	
	pCatA (IRAAPPPLF)	3BP7	−14.31 ± 0.2	3BP4	−14.34 ± 0.17	−0.03 ± 0.37	
pH6	pVIPR (RRKWRRWHL)	1OF2	−17.50 ± 0.26	1OGT_A	−18.66 ± 0±23	−1.16 ± 0.49	
				1OGT_B	−19.85 ± 0.57		
	m9 (GRFAAAIAK)	1K5N	−13.23 ± 0.34	1JGE	−14.22 ± 0.18	−0.99 ± 0.52	
	TIS (RRLPIFSRL)	1W0W	−16.40 ± 0.05	1W0V	−14.18 ± 0.09	2.23 ± 0.14	
	pLMP2(RRRWRRLTV)	1UXW	−16.31 ± 0.01	1UXS	−19.08 ± 0.20	−2.77 ± 0.21	
	pCatA (IRAAPPPLF)	3BP7	−16.30 ± 0.1	3BP4	−16.57 ± 0.94	−0.27 ± 1.04	
pH7[a]	pVIPR (RRKWRRWHL)	1OF2	−17.69 ± 0.30	1OGT_A	−19.03 ± 0.11	−1.34 ± 0.41	−1.65 ± 1.00
				1OGT_B	−20.50 ± 0.21		
	m9 (GRFAAAIAK)	1K5N	−13.60 ± 0.16	1JGE	−14.95 ± 0.06	−1.35 ± 0.22	−4.07 ± 0.45
	TIS (RRLPIFSRL)	1W0W	−16.40 ± 0.02	1W0V	−15.62 ± 0.01	0.77 ± 0.03	0.48 ± 0.33
	pLMP2(RRRWRRLTV)	1UXW	−16.23 ± 0.10	1UXS	−19.12 ± 0.44	−2.90 ± 0.54	−1.00 ± 0.74
	pCatA (IRAAPPPLF)	3BP7	−16.40 ± 0.04	3BP4	−16.45 ± 0.20	−0.05 ± 0.24	Data not available in literature

Experimental [51] allele-wise differences of thermal peptide unbinding parameters are available for pH 7.5 only (for 1OGT, A & B forms refer to the canonical and non-canonical peptide conformations, respectively)

[a] Units are converted to kcal/mol for consistency

in all the retained poses, RMSD values are below 1.5 Å, they are all considered to be successful.

In addition to RMSD, Autodock 4.2 also estimates a FEB score (ΔG) which gives a measure of how favorable a binding event is. A negative FEB value indicates that binding of a peptide is thermodynamically favorable. FEB scores may therefore be used to discriminate between peptide binders or strong binders from non-binders or weak binders. FEB scores for each pH and peptide/allele combination are given in Table 2 and Supplementary Figure 2.

The last column of Table 2 lists the allele-wise differences of the experimentally determined thermal peptide unbinding parameters for pH 7.5 by Narzi, et al. ([51], except for pCatA peptide). Accordingly, the negative values indicate that B*27:05/peptide complex is more stable when compared with the B*27:09/peptide complex. Although being related to stability rather than FEB directly, in their further experiments they have also showed that the differences in the FEB were in good agreement with these destabilization energy differences. Based on this, this observed tendency can be reflected on the FEB profiles as; TIS peptide is bound more strongly by HLA-B*27:09 whereas pVIPR, m9 and pLMP2 peptides are bound more strongly by HLA-B*27:05. A similar tendency is also observed in Autodock 4.2 FEB results obtained in this work (except for pCatA peptide for which no experimental information is available) (Table 2; Fig. 3). For the structures bound to pVIPR further stabilization is achieved in non-canonical conformation with an additional salt bridge formation among Asp116 and pArg5 [51]. This is due to the orientation of pArg5 towards the binding groove instead of being exposed to the solvent as in the canonical pose.

It should be taken into account that, experimental binding energy values given for pLMP2 and pVIPR peptides by Narzi et al. [51] (data not shown in Table 2) are somewhat different than the Autodock 4.2 FEB values. This value clearly indicates a higher stabilization effect of peptide binding to the MHC molecule than the docking predictions. In comparison to other more rigorous dynamic methods involving thermodynamic pathways such as Potential of Mean Force or Alchemical Transformations [52], FEB values obtained from Autodock simulations tend to be less accurate since entropic contribution of receptor flexibility and solvation/desolvation effects are taken into account in a semi-empirical manner [53]. This limitation of the docking method has likely caused a discrepancy in the magnitude of FEB difference values.

An increase in Autodock 4.2 FEB scores was observed for most of the complexes as the pH was decreased to 5, implying a reduced peptide binding affinity in a slightly

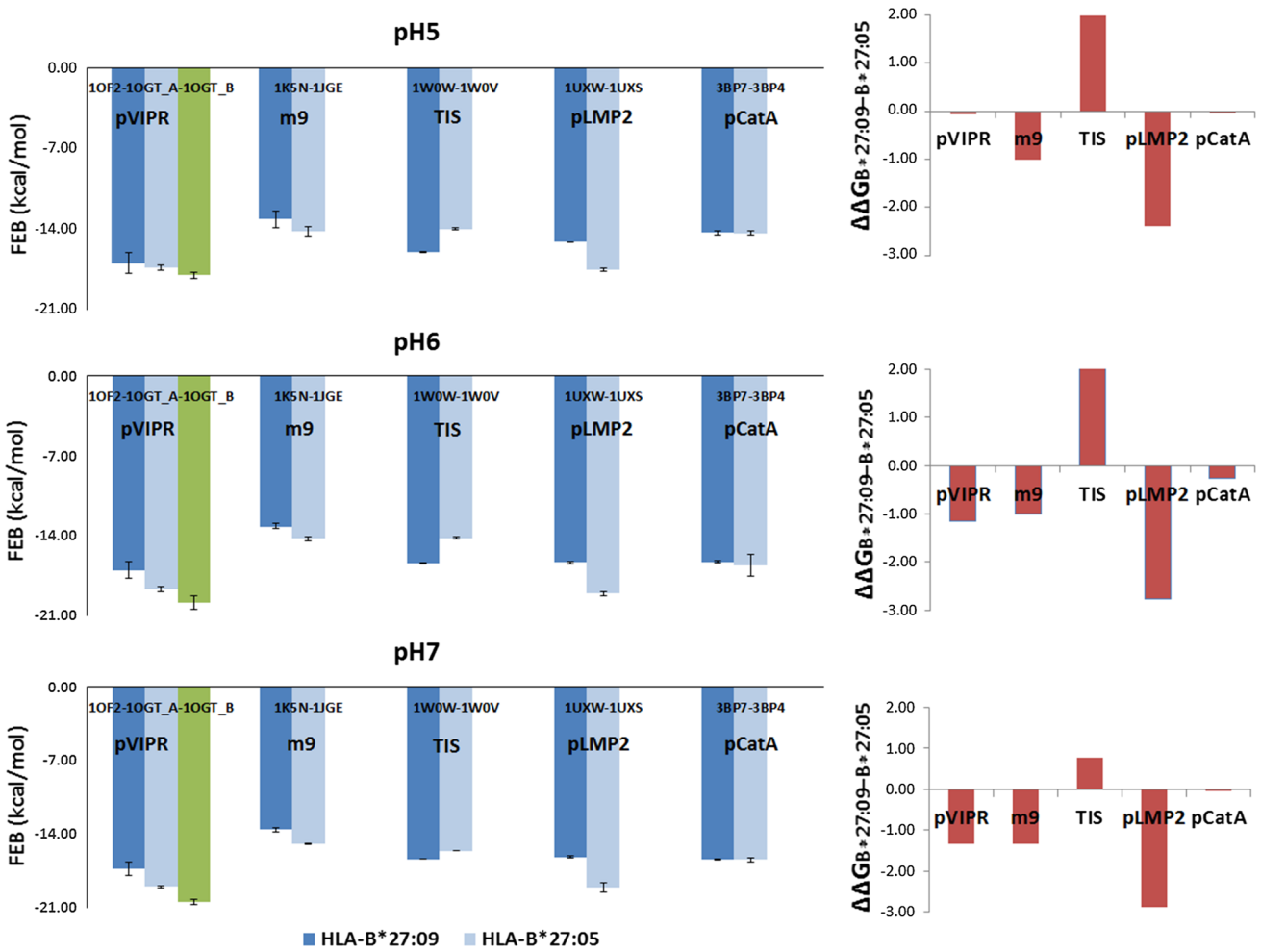

Fig. 3 Allele-wise comparison of the FEB obtained from Autodock 4.2 for the redocking of HLA-B*27:05 and HLA-B*27:09 structures at different pHs. The average of four docking results were taken, standard deviations are shown with *error bars*. The differences ($\Delta\Delta G_{B*27:09\text{-}B*27:05}$) (kcal/mol) are shown in *red column bars* for each pH condition adjacent to the figures

acidic environment for both HLA-B27 structures. The differences in binding affinities between the alleles are also conserved at lower pH (Fig. 3 and Supplementary Figure 2).

Peptide Library Docking at Varying pH Conditions

The results from the previous section suggest a peptide and allele independent decrease in the FEB with decreasing pH. However, the interactions between the binding groove and peptide amino acids at different pH may also depend on the sequence of the peptide. For this reason, we applied this docking procedure to the docking of a virtual combinatorial peptide library onto selected template structures, 1OF2 and 1OGT (A&B) [43], at three pH values: 5.0, 6.0 and 7.0. A total of 1548 docking simulations were performed (for each pH and sub-type combination). Each peptide was docked separately into their respective rigid binding site. Dockings were performed after the adjustment of protonation states of the affected residues using ProPka [45]. For each peptide residue position, a normalized FEB derived from the output of Autodock 4.2 was computed as described in the "Materials and methods" section.

Comparisons of the normalized FEB values are given in Fig. 4 as heat maps and are further detailed in Supplementary Figures 3–5 as column graphs representing the value of each docking. The FEB values used to construct these figures are also given in Supplementary Tables 6–8 in detail. For comparison, an experimental amino acid preference matrix was also constructed based on normalized positional occurrence frequencies of each naturally occurring amino acid in the nonameric peptide binding data for both sub-types retrieved from the Immune Epitope Database (IEDB [47], and Schittenhelm et al. [48] (Fig. 5). As observed in Fig. 5, for the two major peptide anchor

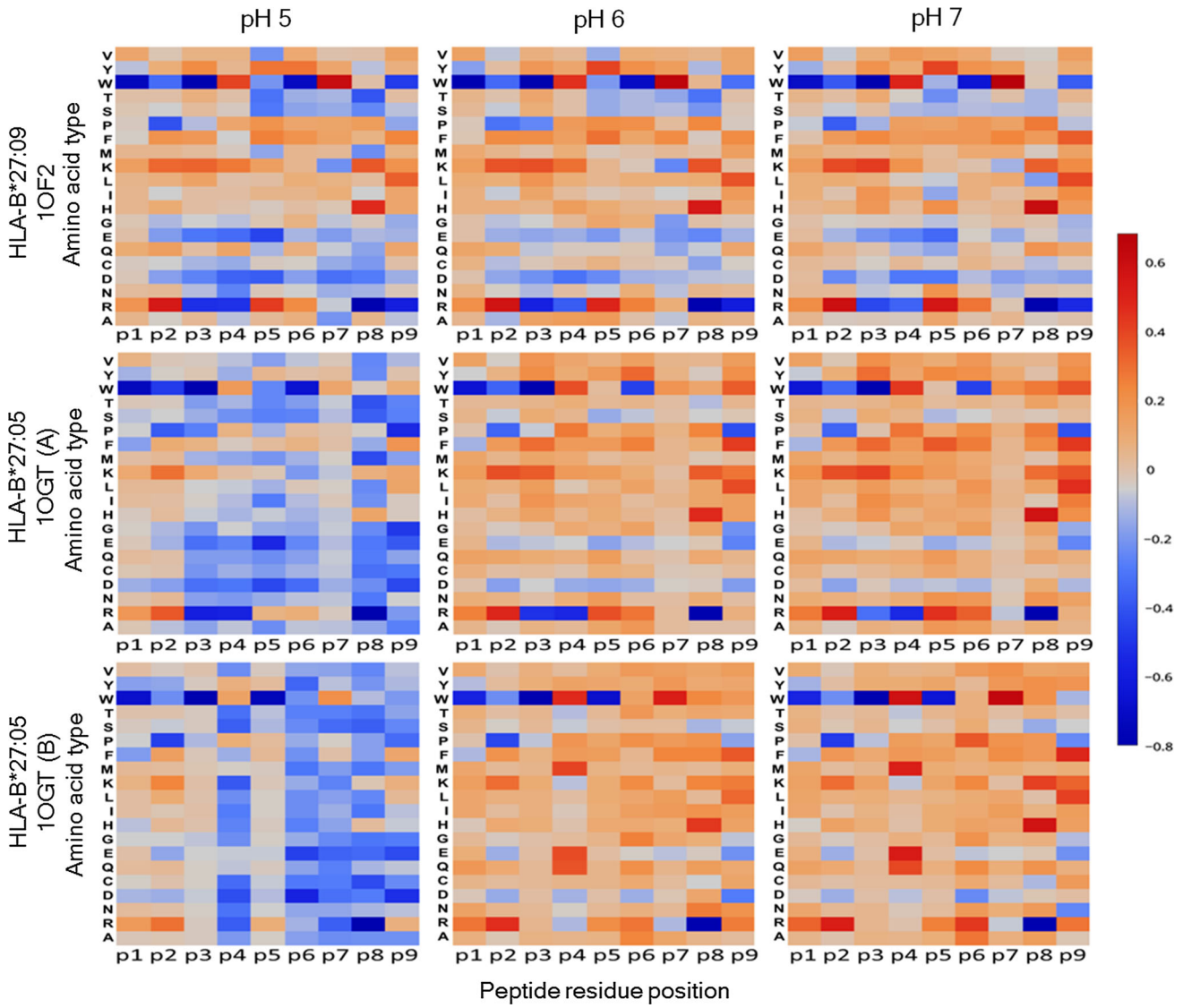

Fig. 4 Amino acid preferences of each peptide position given in a heat map form based on the normalized FEB data obtained from Autodock 4.2. *Positive values* (*red*) indicate a preference for the given amino acid at the respective position. *Negative values* (*blue*) indicate a non-preference for the given amino acid at the respective position

positions, P2 and P9, both sub-types have a very strong preference for Arg and hydrophobic or aromatic amino acids (such as Leu and Phe), respectively.

Showing a canonical conformation when bound to B*27:09, pVIPR is known to show dual conformation, both canonical (A) and non-canonical (B), when bound to B*27:05 [43]. The dual peptide presentation mode in B*27:05 is due to both HLA-B27 subtype-specific amino acid exchange (His116Asp) and the combined presence of Asp116 and Arg at P5, forming a salt bridge in between, altering the shape and charge distribution of the peptide center (Supplementary Figure 1). Apart from the peptide conformations, the rest of the structures (heavy chain and β_2m) are indistinguishable in B*27:05. In both conformations, peptides are anchored at P2 and P9. Peptide positions P1, P2, P8 and P9 are identical whereas the side chains of the central section (P3 to P7), which play a role in TCR recognition are positioned differently [43]. Both conformations are known to occur under physiological conditions [54], while the relevance of the observed difference with regard to AS is still not fully understood [54, 55]. The observance of pVIPR specific T cells are very rare in B*27:09 individuals, while being abundant in healthy B*27:05 individuals and are very frequently present in patients suffering from AS [56]. In B*27:05, the simultaneous occurrence of both peptide modes could be static or dynamic, which could only be clarified through some more advanced experimental methods [43]. The possibility of dynamic occurrence of both conformations within the binding groove might be the prohibiting factor in the high

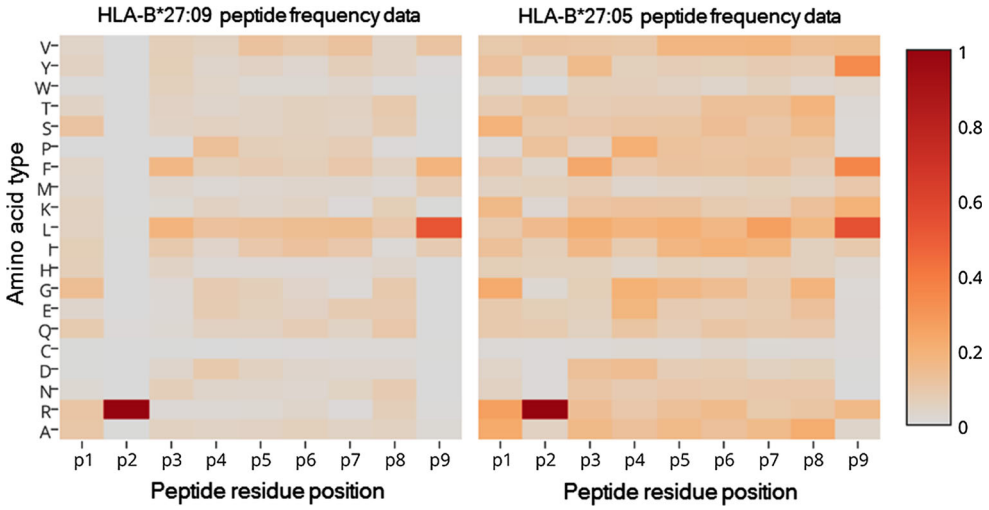

Fig. 5 Amino acid preferences of each peptide position given in a heat map form based on the data retrieved from the Immune Epitope Database (IEDB) [47] and from Schittenhelm et al. [18]. Higher values (*darker red*) indicate a preference for the given amino acid at the respective position

affinity interactions with CDR3 regions of TCR for B*27:05.

Our dockings were carried out on the peptides exhibiting both conformations. The results display very similar amino acid preferences for most of the positions. The only major difference is observed for peptide positions P5 and P6. While Tyr is acceptable in P5 for canonical conformation, it is strictly not preferred for non-canonical conformation. Similarly, Tyr is acceptable in P6 for non-canonical conformation, while it is strictly not preferred in canonical conformation. This is due to the differences in the orientations of P5 and P6 in these two conformations.

P2, the main anchor residue of the peptide, interacts with pocket B, which is a hydrophobic pocket that is surrounded by negatively charged amino acids. Hence, positively charged amino acids with long side chains are preferred to complement the pocket properties involving Glu45 and Cys67 [57, 58]. In this position, there is almost an absolute requirement for Arg [58]. In all pH conditions, our results are inline with these findings. At P9, our predictions at neutral pH match the experimentally observed behavior of amino acid preferences well: Lys, Leu and Phe were predicted as preferred amino acids for both sub-types. Tyr was predicted as a preferred amino acid only for HLA-B*27:05 which is in agreement with the experimental profiles.

For P1, which is the secondary anchor position, small or basic (Gly, Ala, Ser, Lys and Arg) amino acids are highly preferred to interact with pocket A [48]. In this position, Lys and Arg were predicted as preferred amino acids. The middle section of a peptide (P3–P8) usually bulges out into the solvent and makes contacts with the T-cell Receptor in the canonical conformation. Therefore, these positions have less significant restrictions in terms of amino acid preference [59].

Except for P9 (for which Phe appears to be favored over the original peptide sequence Leu by the HLA-B*27:05),

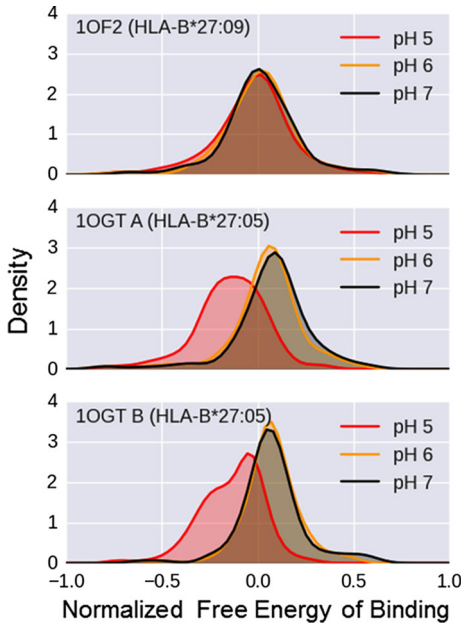

Fig. 6 Distributions of Autodock FEB values for each sub-type and pH combination. The *curves* denote kernel density estimations (KDE) of FEB values generated by using a Gaussian kernel function

the residues of the original peptide sequence almost always appears as the most preferred residue at each position, indicating a clear bias toward the template peptide sequence. This is an expected behavior as the binding groove was kept rigid in its crystallized state in the docking simulations in order to limit the computational burden. It should also be noted that only a limited number of peptide sequences could be simulated, changing only one position while keeping the rest constant. An unbiased and a more complete search could have been achieved with a systematic mutation of all positions at all times leading to 5.12E+11 ($20^9 - 1$) peptide sequences and docking these peptides to calculate the binding scores of each, which has

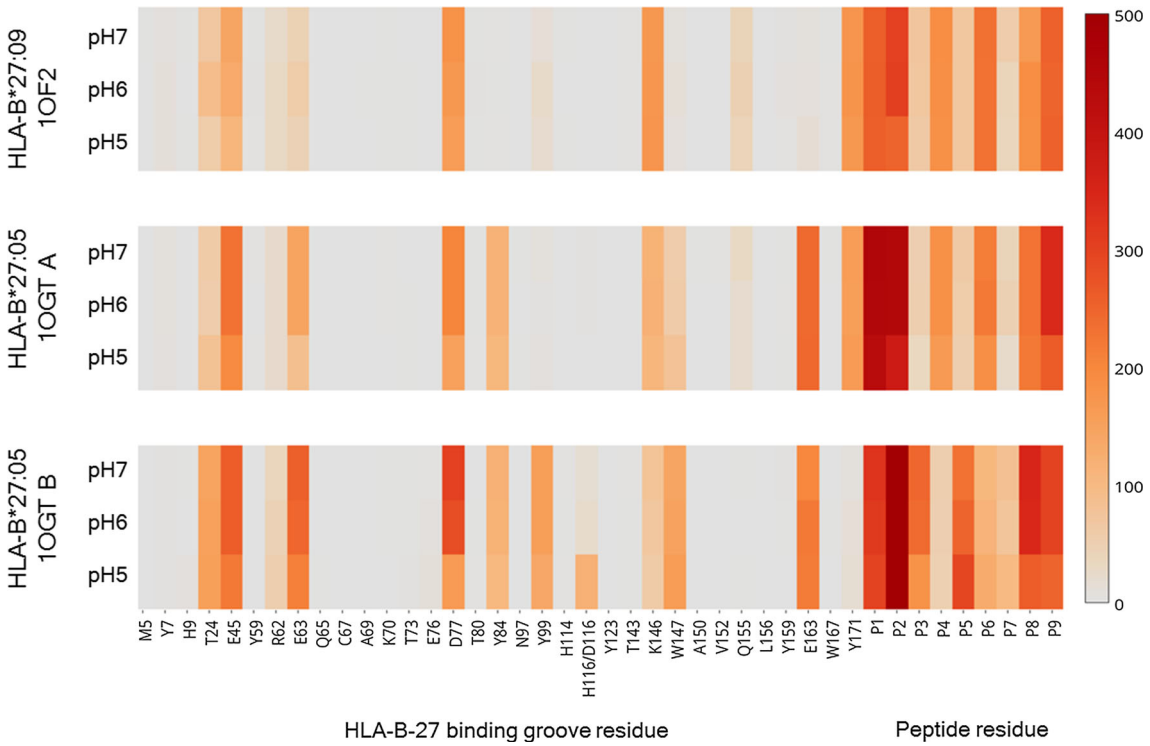

Fig. 7 Strengths of hydrogen bonding interactions between selected binding groove residues in HLA-B*27:05 and HLA-B*27:09 proteins and residue positions in the complexed pVIPR peptide at varying pH conditions in heat map form. Each cell refers to the total number of hydrogen bonds each binding groove amino acid makes with all peptide residues or the total number of hydrogen bonds each peptide amino acid makes with all binding groove residues in a library of 172 docking results (per pH and sub-type)

a very high computational cost. Nevertheless, this limitation of our method did not greatly affect our results, as the rest of the amino acid preferences match the experimentally known profiles.

As the pH is lowered, the capacity to bind peptides in the library is lost (Fig. 4) for both sub-types, while this observation is more drastic for HLA-B*27:05 for both conformations. HLA-B*27:09 allele presenting pVIPR more efficiently than HLA-B*27:05 [56] is also the one that is affected from low pH less. In order to see the overall effect of pH change on peptide-binding behavior of the two sub-types more clearly, we plotted the distribution of the normalized FEB values in Fig. 6, which is also parallel to the profiles observed in the heat maps.

Hydrogen bond analysis on docked structures

The normalized FEB profiles from the previous section give indications of binding affinities for each peptide in the respective peptide library; however, the question of which binding groove residues contribute to the differential pH sensitivity cannot be answered by the FEB values alone. In order to answer this question, we computed the hydrogen bonding interactions between peptide and binding groove residues in each of the docked complexes using HBonanza (see "Materials and methods" section for details). Results are shown in Fig. 7 in a heat map form. The figure shows either the total number of hydrogen bonds each binding groove amino acid makes with all peptide residues or the total number of hydrogen bonds each peptide amino acid makes with all binding groove residues in a library of 172 docking results (per pH and sub-type).

HLA-B*27:05, having enhanced binding properties when compared to B*27:09, has improved hydrogen bonding in the primary anchor positions, P2 and P9, and the secondary anchor position, P1. These anchor positions display the highest difference in terms of hydrogen bonding among the two alleles. The binding pocket residues that interact with these peptide positions are mainly the B pocket residues Thr24, Glu45, Glu63 and Glu163 (interacting with P2), the F-pocket residues Asp77, Thr84 and Trp147 that frame the polymorphic residue 116 (Asp/His) (interacting with P8 and P9) and the A pocket residues Glu63 and Glu163 (interacting with P1). A closer look at the H bonding profiles (Fig. 7) of these binding groove residues direct us to the residues responsible from this behavior. Thr24, Glu45, Glu63, Asp77, Thr84, Trp147 and Glu163 display increased H bonding in HLA-B*27:05 alleles corresponding to the increased binding of P1, P2 and P9. The differences between these interactions among

the HLA-B*27:05 and HLA-B*27:09 structures hint at an allele dependent behavior. Although the primary anchor site, P2, is far from the polymorphic residue 116, it is also affected through the electrostatic interactions [51].

For the dual conformation observed in HLA-B*27:05 allele, the orientations of the peptide side chains differ only from P3 to P7, which is reflected on the H bonding profiles as in engagement in different H bonds. Mainly, the differences occurring around P5 are responsible from the observed changes in the H bonding profiles. In the non-canonical mode (B); P4 and P6 are exposed to solvent, while P5 is locked within the binding groove different from the canonical mode. Hence, in the canonical mode, while P4 and P6 are actively forming H bonds; in the non-canonical mode, P3 and P5 take over this mission.

As pH increases from 5 to 7, H bonding also increases leading to better binding for both HLA-B*27:05 and HLA-B*27:09 structures. This affect is observed to be more dominant for HLA-B*27:05. Especially, Glu45, Glu63 and Asp77 display an increase in H bonding with increasing pH. Among these, Glu63 and Asp77 change their protonation states (become protonated) when pH is lowered, while Glu45 is always deprotonated, not showing any variations (data not shown in the SI Table 1 for simplicity). Based on these, the protonation state variations of Glu63 (interacting with P2) and Asp77 (interacting with P9) can be considered to be playing a leading role in the observed profile shifts due to pH.

Our study hints at a higher sensitivity of the HLA-B*27:05 allele for peptide-binding at acidic pH levels than the HLA-B*27:09 allele. This may imply that HLA-B*27:09 has a better capability to perform cross-presentation by binding peptides in endosomes and/or exchange peptides in the slightly acidic Trans-Golgi Network. As a result, HLA-B*27:09 allele may have a better chance of being present on the surface of Antigen Presenting Cells and thereby inducing a CD8+ T-cell response, providing a possible explanation for the differential association of the two alleles with AS. Having conducted computational docking only, a full and a more informative picture could only be obtained when the results of our study are combined with further experimental studies including HLA-peptide-TCR complexes. Here, in order to build a framework for understanding the mechanisms of MHC I peptide selection at varying pH conditions, we have simplified this complex system to HLA-peptide and hence excluded all the other factors influencing peptide binding (such as nature of peptide supply, chaperone molecules, TCR binding).

Nevertheless, our results should be viewed with caution as well, mainly for two reasons. First, we studied only single amino-acid substitutions of a template peptide sequence. A more comprehensive picture could have been obtained when a larger ensemble of possible peptide binders are included. Second, we assumed rigid binding groove conformations and did not include an analysis on dynamics of the generated complexes. These factors should be taken into account for the validation of our findings.

Conclusion

In the present study, our observations offer a general view on the amino acid preferences of the pVIPR peptide docked to HLA-B*27:05 and HLA-B*27:09 at varying pH conditions (pH 5.0, 6.0 and 7.0). Using X-ray structures retrieved from the PDB [1OF2 and 1OGT (A&B)], a combinatorial peptide library was built using a single amino acid mutation principle and docked into the unbound protein structures. A systematic structural analysis was used to investigate the results based on the FEBs. From the obtained results, it is evident that peptide-HLA complexes are less stable as the pH is lowered and an enhanced peptide binding strength in the B*27:05 allele is observed regardless of the pH condition. Low pH destabilizes HLA-peptide complexes by influencing the protonation states of some Asp, Glu and His residues, as expected. However, HLA-B*27:05 is much more affected while the binding energy profile of HLA-B*27:09 is affected less. In addition to the known polymorphism among the alleles, hydrogen bonding suggests that the interaction between the main anchor position P2 and its respective binding pocket residue Glu63 and P9 and its respective binding pocket residue Asp77 is affected from pH the most, causing an overall shift in the FEB profiles.

Although the direct role of pVIPR in AS cannot be completely enlightened with the current computational findings, the observed differences in pVIPR binding in individuals with HLA-B*27:05 and HLA-B*27:09 provide informative insights into peptide presentation and might hint on the inappropriate T cell selection by individuals with the disease-associated HLA-B27 subtype. The existence of high number of pVIPR-specific CTLs in some B*27:05 individuals [56] might be related to the cross-reactivity of TCR which causes selective increase. The allele-dependent dynamics and different conformational states of pVIPR bound to HLA may play a role in the context of molecular mimicry and in the differential association of HLA-B27 subtypes with AS [26, 60]. The buried polymorphism and an additional dual peptide presentation mode features of the disease associated B*27:05 allele can hence be linked to the course of the development of AS. However, the conclusions related to AS cannot go beyond being speculative since the complete structure of HLA-B27-pVIPR-TCR complex is not currently present.

Acknowledgments This work was supported by TUBITAK under Grant 113M293.

Compliance with ethical standards

Conflict of interest No conflicting financial interests exist.

References

1. Abbas AK, Lichtman AH, Pillai S (2012) Cellular and molecular immunology, 7th edn. Elsevier/Saunders, Philadelphia
2. Hulpke S, Tampé R (2013) The MHC I loading complex: a multitasking machinery in adaptive immunity. Trends Biochem Sci 38:412–420. doi:10.1016/j.tibs.2013.06.003
3. Bevan MJ (1976) Cross-priming for a secondary cytotoxic response to minor H antigens with H-2 congenic cells which do not cross-react in the cytotoxic assay. J Exp Med 143:1283–1288. http://www.ncbi.nlm.nih.gov/pmc/articles/PMC2190184/
4. Rock KL, Gamble S, Rothstein L (1990) Presentation of exogenous antigen with class I major histocompatibility complex molecules. Science 249(4971):918–921
5. Heath WR, Carbone FR (2001) Cross-presentation, dendritic cells, tolerance and immunity. Annu Rev Immunol 19:47–64. doi:10.1146/annurev.immunol.19.1.47
6. Sigal LJ, Crotty S, Andino R, Rock KL (1999) Cytotoxic T-cell immunity to virus-infected non-haematopoietic cells requires presentation of exogenous antigen. Nature 398(6722):77–80. doi:10.1038/18038
7. Rock KL, Shen L (2005) Cross-presentation: underlying mechanisms and role in immune surveillance. Immunol Rev 207:166–183. doi:10.1111/j.0105-2896.2005.00301.x
8. Di Pucchio T, Chatterjee B, Smed-Sörensen A, Clayton S, Palazzo A, Montes M, Xue Y, Mellman I, Banchereau J, Connolly JE (2008) Direct proteasome-independent cross-presentation of viral antigen by plasmacytoid dendritic cells on major histocompatibility complex class I. Nat Immunol 9:551–557. doi:10.1038/ni.1602
9. Geisow MJ, Evans WH (1984) pH in the endosome. Measurements during pinocytosis and receptor-mediated endocytosis. Exp Cell Res 150(1):36–46. http://www.ncbi.nlm.nih.gov/pubmed/6198190
10. Rötzschke O, Lau JM, Hofstätter M, Falk K, Strominger JL (2002) A pH-sensitive histidine residue as control element for ligand release from HLA-DR molecules. Proc Natl Acad Sci USA 99:16946–16950. doi:10.1073/pnas.212643999
11. Deutsch C, Taylor JS, Wilson DF (1982) Regulation of intracellular pH by human peripheral blood lymphocytes as measured by 19F NMR. Proc Natl Acad Sci USA 79(24):7944–7948. http://www.ncbi.nlm.nih.gov/pubmed/6961462
12. Reich Z, Altman JD, Boniface JJ, Lyons DS, Kozono H, Ogg G, Morgan C, Davis MM (1997) Stability of empty and peptide-loaded class II major histocompatibility complex molecules at neutral and endosomal pH: comparison to class I proteins. Proc Natl Acad Sci USA 94(6):2495–2500. http://www.ncbi.nlm.nih.gov/pubmed/9122223
13. Amigorena S, Savina A (2010) Intracellular mechanisms of antigen cross presentation in dendritic cells. Curr Opin Immunol 22:109–117. doi:10.1016/j.coi.2010.01.022
14. Delamarre L, Pack M, Chang H, Mellman I, Trombetta ES (2005) Differential lysosomal proteolysis in antigen-presenting cells determines antigen fate. Science (New York, NY) 307:1630–1634. doi:10.1126/science.1108003
15. Mantegazza AR, Savina A, Vermeulen M, Pérez L, Geffner J, Hermine O, Rosenzweig SD, Faure F, Amigorena S (2008) NADPH oxidase controls phagosomal pH and antigen cross-presentation in human dendritic cells. Blood 112:4712–4722. doi:10.1182/blood-2008-01-134791
16. Savina A, Jancic C, Hugues S, Guermonprez P, Vargas P, Moura IC, Lennon-Duménil A-M, Seabra MC, Raposo G, Amigorena S (2006) NOX2 controls phagosomal pH to regulate antigen processing during crosspresentation by dendritic cells. Cell 126:205–218. doi:10.1016/j.cell.2006.05.035
17. Gromme M, Uytdehaag FG, Janssen H, Calafat J, van Binnendijk RS, Kenter MJ, Tulp A, Verwoerd D, Neefjes J (1999) Recycling MHC class I molecules and endosomal peptide loading. Proc Natl Acad Sci USA 96(18):10326–10331. http://www.ncbi.nlm.nih.gov/pmc/articles/PMC17887/
18. Stryhn A, Pedersen LO, Romme T, Olsen AC, Nissen MH, Thorpe CJ, Buus S (1996) pH dependence of MHC class I-restricted peptide presentation. J Immunol (Baltimore, Md: 1950) 156:4191–4197. http://www.jimmunol.org/content/156/11/4191.full.pdf
19. Ma W, Van den Eynde BJ (2014) Endosomal compartment: also a dock for MHC class I peptide loading. Eur J Immunol 44:650–653. doi:10.1002/eji.201444470
20. Wälchli S, Kumari S, Fallang L-E, Sand KMK, Yang W, Landsverk OJB, Bakke O, Olweus J, Gregers TF (2014) Invariant chain as a vehicle to load antigenic peptides on human MHC class I for cytotoxic T-cell activation. Eur J Immunol 44:774–784. doi:10.1002/eji.201343671
21. Duan F, Srivastava PK (2012) An invariant road to cross-presentation. Nat Immunol 13:207–208. doi:10.1038/ni.2235
22. Sorrentino R, Bockmann RA, Fiorillo MT (2014) HLA-B27 and antigen presentation: at the crossroads between immune defense and autoimmunity. Mol Immunol 57(1):22–27. doi:10.1016/j.molimm.2013.06.017
23. Bettosini F, Fiorillo MT, Magnacca A, Leone L, Torrisi MR, Sorrentino R (2005) The C terminus of the nucleoprotein of influenza A virus delivers antigens transduced by Tat to the trans-golgi network and promotes an efficient presentation through HLA class I. J Virol 79:15537–15546. doi:10.1128/JVI.79.24.15537-15546.2005
24. Magnacca A, Persiconi I, Nurzia E, Caristi S, Meloni F, Barnaba V, Paladini F, Raimondo D, Fiorillo MT, Sorrentino R (2012) Characterization of a proteasome and TAP-independent presentation of intracellular epitopes by HLA-B27 molecules. J Biol Chem 287:30358–30367. doi:10.1074/jbc.M112.384339
25. Leonhardt RM, Fiegl D, Rufer E, Karger A, Bettin B, Knittler MR (2010) Post-endoplasmic reticulum rescue of unstable MHC class I requires proprotein convertase PC7. J Immunol 184(6):2985–2998. doi:10.4049/jimmunol.0900308
26. Ramos M, Lopez de Castro JA (2002) HLA-B27 and the pathogenesis of spondyloarthritis. Tissue Antigens 60(3):191–205. http://www.ncbi.nlm.nih.gov/pubmed/12445302
27. Ziegler A, Loll B, Misselwitz R, Uchanska-Ziegler B (2009) Implications of structural and thermodynamic studies of HLA-B27 subtypes exhibiting differential association with ankylosing spondylitis. Adv Exp Med Biol 649:177–195. http://www.ncbi.nlm.nih.gov/pubmed/19731629
28. Uchanska-Ziegler B, Loll B, Fabian H, Hee CS, Saenger W, Ziegler A (2012) HLA class I-associated diseases with a suspected autoimmune etiology: HLA-B27 subtypes as a model system. Eur J Cell Biol 91(4):274–286. doi:10.1016/j.ejcb.2011.03.003
29. Brewerton DA, Hart FD, Nicholls A, Caffrey M, James DC, Sturrock RD (1973) Ankylosing spondylitis and HL-A 27. Lancet 1(7809):904–907. http://www.ncbi.nlm.nih.gov/pubmed/4123836
30. Ohno S, Ohguchi M, Hirose S, Matsuda H, Wakisaka A, Aizawa M (1982) Close association of HLA-Bw51 with Behcet's disease. Arch Ophthalmol 100(9):1455–1458. http://www.ncbi.nlm.nih.gov/pubmed/6956266

31. Lafuente EM, Reche PA (2009) Prediction of MHC-peptide binding: a systematic and comprehensive overview. Curr Pharm Des 15(28):3209–3220. http://www.ncbi.nlm.nih.gov/pubmed/19860671
32. Tong JC, Tan TW, Ranganathan S (2007) Methods and protocols for prediction of immunogenic epitopes. Brief Bioinform 8(2):96–108. doi:10.1093/bib/bbl038
33. Liao WW, Arthur JW (2011) Predicting peptide binding to major histocompatibility complex molecules. Autoimmun Rev 10(8):469–473. doi:10.1016/j.autrev.2011.02.003
34. Lin HH, Ray S, Tongchusak S, Reinherz EL, Brusic V (2008) Evaluation of MHC class I peptide binding prediction servers: applications for vaccine research. BMC Immunol 9:8. doi:10.1186/1471-2172-9-8
35. Peters B, Bui HH, Frankild S, Nielson M, Lundegaard C, Kostem E, Basch D, Lamberth K, Harndahl M, Fleri W, Wilson SS, Sidney J, Lund O, Buus S, Sette A (2006) A community resource benchmarking predictions of peptide binding to MHC-I molecules. PLoS Comput Biol 2(6):e65. doi:10.1371/journal.pcbi.0020065
36. Berman H, Henrick K, Nakamura H (2003) Announcing the worldwide Protein Data Bank. Nat Struct Biol 10(12):980. doi:10.1038/Nsb1203-980
37. Patronov A, Dimitrov I, Flower DR, Doytchinova I (2012) Peptide binding to HLA-DP proteins at pH 5.0 and pH 7.0: a quantitative molecular docking study. BMC Struct Biol 12:20. doi:10.1186/1472-6807-12-20
38. Damato M, Fiorillo MT, Carcassi C, Mathieu A, Zuccarelli A, Bitti PP, Tosi R, Sorrentino R (1995) Relevance of residue-116 of Hla-B27 in determining susceptibility to ankylosing-spondylitis. Eur J Immunol 25(11):3199–3201. doi:10.1002/eji.1830251133
39. Khan MA (2002) Update on spondyloarthropathies. Ann Intern Med 136(12):896–907. http://www.ncbi.nlm.nih.gov/pubmed/12069564
40. Falk K, Rotzschke O, Stevanovic S, Jung G, Rammensee HG (1991) Allele-specific motifs revealed by sequencing of self-peptides eluted from MHC molecules. Nature 351(6324):290–296. doi:10.1038/351290a0
41. Pohlmann T, Bockmann RA, Grubmuller H, Uchanska-Ziegler B, Ziegler A, Alexiev U (2004) Differential peptide dynamics is linked to major histocompatibility complex polymorphism. J Biol Chem 279(27):28197–28201. doi:10.1074/jbc.C400128200
42. Morris GM, Huey R, Lindstrom W, Sanner MF, Belew RK, Goodsell DS, Olson AJ (2009) AutoDock4 and AutoDockTools4: automated docking with selective receptor flexibility. J Comput Chem 30(16):2785–2791. doi:10.1002/Jcc.21256
43. Hulsmeyer M, Fiorillo MT, Bettosini F, Sorrentino R, Saenger W, Ziegler A, Uchanska-Ziegler B (2004) Dual, HLA-B27 subtype-dependent conformation of a self-peptide. J Exp Med 199(2):271–281. doi:10.1084/jem.20031690
44. The PyMOL Molecular Graphics System Vrp, Schrödinger, LLC
45. Sondergaard CR, Olsson MHM, Rostkowski M, Jensen JH (2011) Improved treatment of ligands and coupling effects in empirical calculation and rationalization of pK(a) values. J Chem Theory Comput 7(7):2284–2295. doi:10.1021/Ct200133y
46. Patronov A, Dimitrov I, Flower DR, Doytchinova I (2011) Peptide binding prediction for the human class II MHC allele HLA-DP2: a molecular docking approach. BMC Struct Biol 11:32. doi:10.1186/1472-6807-11-32
47. Vita R, Overton JA, Greenbaum JA, Ponomarenko J, Clark JD, Cantrell JR, Wheeler DK, Gabbard JL, Hix D, Sette A, Peters B (2015) The immune epitope database (IEDB) 3.0. Nucleic Acids Res 43(Database issue):D405-412. doi:10.1093/nar/gku938
48. Schittenhelm RB, Sian TCCLK, Wilmann PG, Dudek NL, Purcell AW (2015) Revisiting the arthritogenic peptide theory: quantitative not qualitative changes in the peptide repertoire of HLA-B27 allotypes. Arthritis Rheumatol (Hoboken, NJ) 67:702–713. doi:10.1002/art.38963
49. Durrant JD, McCammon JA (2011) HBonanza: a computer algorithm for molecular-dynamics-trajectory hydrogen-bond analysis. J Mol Graph Model 31:5–9. doi:10.1016/j.jmgm.2011.07.008
50. McDonald IK, Thornton JM (1994) Satisfying hydrogen bonding potential in proteins. J Mol Biol 238(5):777–793. doi:10.1006/jmbi.1994.1334
51. Narzi D, Winkler K, Saidowsky J, Misselwitz R, Ziegler A, Bockmann RA, Alexiev U (2008) Molecular determinants of major histocompatibility complex class I complex stability—shaping antigenic features through short and long range electrostatic interactions. J Biol Chem 283(34):23093–23103. doi:10.1074/jbc.M710234200
52. Wereszczynski J, McCammon JA (2012) Statistical mechanics and molecular dynamics in evaluating thermodynamic properties of biomolecular recognition. Q Rev Biophys 45(1):1–25. doi:10.1017/S0033583511000096
53. Huey R, Morris GM, Olson AJ, Goodsell DS (2007) A semiempirical free energy force field with charge-based desolvation. J Comput Chem 28(6):1145–1152. doi:10.1002/jcc.20634
54. Fabian H, Huser H, Narzi D, Misselwitz R, Loll B, Ziegler A, Bockmann RA, Uchanska-Ziegler B, Naumann D (2008) HLA-B27 subtypes differentially associated with disease exhibit conformational differences in solution. J Mol Biol 376(3):798–810. doi:10.1016/j.jmb.2007.12.009
55. de Castro JAL (2007) HLA-B27 and the pathogenesis of spondyloarthropathies. Immunol Lett 108(1):27–33. doi:10.1016/j.imlet.2006.10.004
56. Fiorillo MT, Maragno M, Butler R, Dupuis ML, Sorrentino R (2000) CD8(+) T-cell autoreactivity to an HLA-B27-restricted self-epitope correlates with ankylosing spondylitis. J Clin Investig 106(1):47–53. doi:10.1172/JCI9295
57. Fiorillo MT, Ruckert C, Hulsmeyer M, Sorrentino R, Saenger W, Ziegler A, Uchanska-Ziegler B (2005) Allele-dependent similarity between viral and self-peptide presentation by HLA-B27 subtypes. J Biol Chem 280(4):2962–2971. doi:10.1074/jbc.M410807200
58. Madden DR, Gorga JC, Strominger JL, Wiley DC (1991) The structure of HLA-B27 reveals nonamer self-peptides bound in an extended conformation. Nature 353(6342):321–325. doi:10.1038/353321a0
59. Fukazawa T, Wang J, Huang F, Wen J, Tyan D, Williams KM, Raybourne RB, Yu DT (1994) Testing the importance of each residue in a HLA-B27-binding peptide using monoclonal antibodies. J Immunol 152(3):1190–1196. http://www.ncbi.nlm.nih.gov/pubmed/8301123
60. Khan MA, Ball EJ (2002) Genetic aspects of ankylosing spondylitis. Best Pract Res Clin Rheumatol 16(4):675–690